Proceedings of the 43rd "Jaszowiec", International School and Conference on the Physics of Semiconductors, Wisła 2014

Properties of Sonochemically Prepared $CuIn_xGa_{1-x}S_2$ and $CuIn_xGa_{1-x}Se_2$

M. Jesionek[a], M. Nowak[a,*], P. Szperlich[a], M. Kępińska[a], K. Mistewicz[a], B. Toroń[a], D. Stróż[b], J. Szala[c] and T. Rzychoń[c]

[a]Solid State Physics Section, Institute of Physics — Center for Science and Education, Silesian University of Technology, Z. Krasińskiego 8, 40-019 Katowice, Poland

[b]Institute of Materials Science, University of Silesia, 75 Pułku Piechoty 1A, 41-500 Chorzów, Poland

[c]Department of Materials Science, Silesian University of Technology, Z. Krasińskiego 8, 40-019 Katowice, Poland

Nanoparticles of chalcopyrites copper indium gallium sulfide ($CuIn_xGa_{1-x}S_2$ or CIGS) and copper indium gallium selenide ($CuIn_xGa_{1-x}Se_2$ or CIGSe) were fabricated sonochemically. They were characterized by X-ray diffraction, scanning electron microscopy, energy dispersive X-ray spectroscopy, high resolution transmission electron microscopy, selected area electron diffraction, and diffuse reflectance spectroscopy. The electrical and photoelectrical properties of the fabricated nanomaterials were investigated.

DOI: 10.12693/APhysPolA.126.1107

PACS: 43.35.Ei, 72.20.Jv, 72.40.+w, 81.07.Bc

1. Introduction

Nanoscale chalcopyrites copper indium gallium sulfide ($CuIn_xGa_{1-x}S_2$ or CIGS) and copper indium gallium selenide ($CuIn_xGa_{1-x}Se_2$ or CIGSe) are semiconductors useful for the manufacture of solar cells, because of the possibilities of large-area production and the significant cost-reduction in device fabrication [1, 2]. Recently [3], these nanomaterials have been surfactant-free synthesized sonochemically at 373 K. This synthetic approach eliminates the need for organic stabilizers, which may act as insulators in the final photovoltaic device, and reduces the number of reaction steps for synthesis of high-quality $Cu(In,Ga)(S,Se)_2$ nanocrystals. With regard to the nanocrystal ink, a simple process for solar cell fabrication by using a non-vacuum technique based on the CIGSe absorber layer was presented [3].

The aim of this paper was to synthesize the CIGSe and CIGS nanomaterials using ultrasound radiation at lower temperature than it was done in [3]. The other goal of this paper was to use the frequency-dependence method of photoconductivity investigations [4, 5] to determine carrier lifetimes in the CIGSe nanomaterials.

2. Experiment

CIGSe and CIGS were synthesized sonochemically at the temperature of 323 K using autotune high intensity ultrasonic processor VCX750 Sonics & Materials equipped with cup horn (f = 20 kHz, P = 300 W). In a typical procedure, CuCl (0.113 g), $In(OAc)_3$ (0.233 g), $Ga(NO_3)_3 \cdot xH_2O$ (0.094 g), and Se powder (0.180 g) were mixed with 12 cm^3 ethylene glycol and 4 cm^3 hydrazine monohydrate (98%). To eliminate the eventual remaining substrates CIGSe sol was five times rinsed with deionized water and centrifuged. Product of this procedure was dried in vacuum (p = 1 mbar) at room temperature (Fig. 1a).

The powder X-ray diffraction (XRD) of the synthesized CIGSe and CIGS was performed on JEOL JDX-7S diffractometer with Cu K_α radiation. Scanning electron investigations and energy dispersive X-ray (EDS) analysis were taken on Hitachi S-4200 microscope with Noran Instruments EDS Voyager 3500 spectrometer. The high-resolution transmission electron microscopy (HRTEM) and selected area electron diffraction (SAED) were performed on JEOL - JEM 3010 microscope.

The optical diffuse reflection spectroscopy (DRS) was carried out on spectrophotometer PC-2000 (Ocean Optics Inc.) equipped with integrating sphere ISP-REF (Ocean Optics Inc.) [6]. The DC electric characteristics were registered in darkness using Keithley 6517A electrometer. The frequency-dependent photoconductivity current was measured using EG&G 5110 lock-in amplifier and acousto-optically modulated Ar laser (λ = 488 nm). Thick films of CIGSe were prepared for these investigations on alumina #103 substrates (Electronics Design Center, Case Western Reserve University) with interdigitated electrodes (preparation details are the same as the presented in [7]). The ohmic behavior of electric current in the investigated samples was evaluated with applied field from –4 kV/m to +4 kV/m. All electric measurements were performed in air conditions at 298 K using LabView programs.

3. Results and discussion

The powder XRD pattern of the sonochemically prepared CIGSe (Fig. 1b) shows well defined, sharp peaks. So, it indicates that the product can be well crystallized. The highest diffraction peaks correspond to the (112) and (220) or (104) as well as (312) or (116) planes of

*corresponding author; e-mail: Marian.Nowak@polsl.pl

$CuIn_{0.85}Ga_{0.15}Se_2$. The identification was done using the PCSIWIN computer program and the data from JCPDS-International Centre for Diffraction Data 2007. However, the additional diffraction peaks show the existence of another crystalline material in the sample. The diffraction peaks a, b, c, and d correspond to CuSe. Therefore, the elemental atomic ratio of 0.24:0.27:0.04:0.45 for Cu, In, Ga and Se determined by EDS investigations cannot be used for determining the molar composition of the synthesized $CuIn_xGa_{1-x}Se_2$.

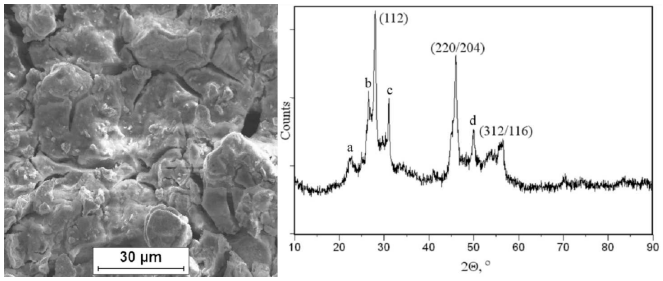

Fig. 1. Typical SEM micrograph (a) and the powder XRD pattern (b) of CIGSe xerogel.

The HRTEM image reveals that the product consists of nanoparticles with average size of 10–15 nm (Fig. 2). The indicated fringe spacings of $d = 0.306(6)$ nm correspond to the interplanar distances between the (112) planes of $CuIn_{0.85}Ga_{0.15}Se_2$ crystal.

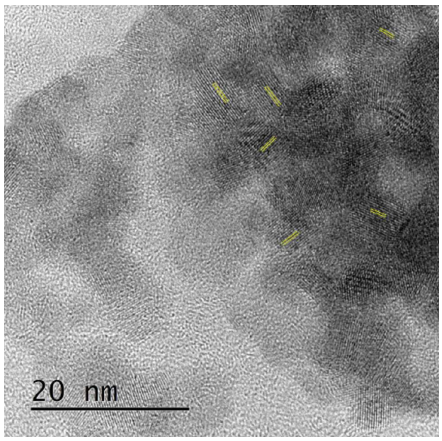

Fig. 2. Typical HRTEM image of CIGSe nanoparticles. The fringe spacings of $d = 0.306(6)$ nm correspond to the interplanar distances between the (112) planes of CIGSe crystal.

Figure 3 presents the diffuse reflectance (R_d) spectrum of prepared CIGSe. Unfortunately, the well-known [8] value ($\approx$ 1.04 eV) of energy gap of CIGSe is behind the spectral range of used experimental setup. The abrupt decrease in R_d when radiation becomes more intensively absorbed with decreasing wavelength corresponds to some optical absorption edge [6] of another component of the sample. The values of R_d were converted to the Kubelka–Munk function (known to be proportional to the absorption coefficient of light in the investigated material (α)) [6]:

$$F_{K-M}(R_d) = \frac{(1-R_d)^2}{2R_d} \sim \alpha. \quad (1)$$

In the case of direct allowed absorption one expects

$$F_{K-M} = \frac{A_1\sqrt{h\nu - E_g}}{h\nu}, \quad (2)$$

where E_g represents the direct allowed energy gap, A_1 is a constant parameter. Therefore Fig. 3 presents the spectrum of F_{K-M} transformed into form of $(F_{K-M}h\nu)^2$. The value of energy gap $E_{g2} = 1.94(1)$ eV was determined by the intersection of the straight-line extrapolations below and above the small photon energy knee of the $(F_{K-M}h\nu)^2$ line. The determined value of E_{g2} is close to the value 2.03 eV known [9] for CuSe thin films. Such interpretation of the observed energy gap E_{g2} is in agreement with the results of XRD investigations.

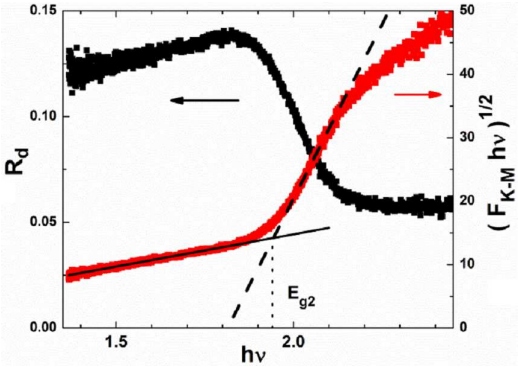

Fig. 3. Spectra of the diffuse reflectance coefficient (black data) and the Kubelka–Munk function (red data) calculated for the DRS data of CIGSe xerogel (dash black line represents the least squares fitted theoretical dependence (2) for direct allowed absorption; solid black line fits the slope of spectral dependence of transformed values of F_{K-M} in small $h\nu$ range; vertical line shows the determined energy gap $E_{g2} = 1.94(1)$ eV (description in the text).

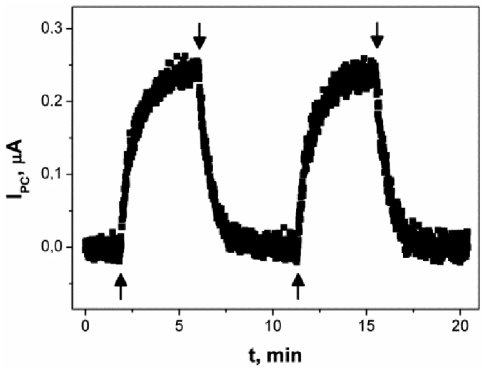

Fig. 4. Photoconductivity current responses on switching on (↑) and switching off (↓) illumination of CIGSe in air ($\lambda = 488$ nm; $P = 50$ mW; $E = 400$ V/m; $T = 298$ K).

Figure 4 presents typical responses of DC photoconductivity current on switching on and switching off illumination of prepared CIGSe thick film. After switching on illumination the electric conductivity current monotonically increases due to photogeneration of excess carriers. When illumination is switched off the current decreases due to recombination of excess carriers (Fig. 4). This is the well-known kinetics of photoconductivity in semiconductors.

Figure 5 shows photoconductivity current in CIGSe as a function of frequency (f) of illumination chopping. The results were least-squares fitted with the following dependence:

$$I_{\mathrm{PC}} = \frac{A}{\sqrt{1+(2\pi f\tau)^2}} + \frac{B}{f}, \tag{3}$$

where the first term describes influence of carrier lifetime (τ) on photoconductivity response [4] and the second term presents so-called $1/f$ noises in photoconductivity current [10]. The origin of the $1/f$ noises is not well-known. It is assumed that metastable electron traps and crystal defects in photodetectors and in their interfaces are responsible for these noises [5].

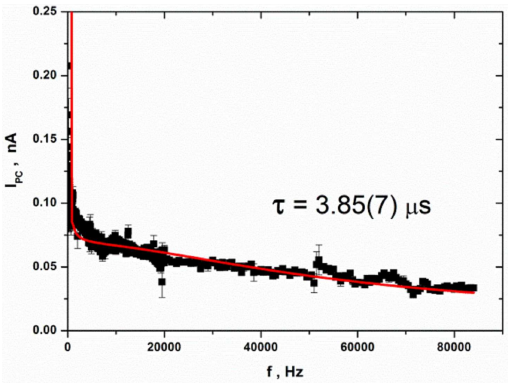

Fig. 5. Frequency dependence of photoconductivity current flowing through the fabricated CIGSe sample. Solid curve represents relation (3) calculated for the least-squared fitted values of $A = 6.71(4) \times 10^{-11}$ A, $B = 1.55(8) \times 10^{-8}$ A/s, and $\tau = 3.85(7) \times 10^{-6}$ s.

The fitting of the photoconductivity data with Eq. (3) is rather good. However, the determined carrier lifetime $\tau = 3.85(7) \times 10^{-6}$ s is relatively large (in comparison with literature data on CIGSe). Time-resolved photoluminescence measurements on polycrystalline CIGSe thin films corresponding to high-efficiency solar cells indicated recombination lifetimes as long as 250 ns [11]. Hence, the appropriate investigations are necessary in the future.

4. Conclusions

In summary, very simple, sonochemical synthesis of CIGSe and CIGS nanophases can be performed in relatively low temperature. It is a convenient, fast, mild and efficient route for producing CIGSe and CIGS nanopowders. The XRD, HRTEM and SAED patterns show that the as-prepared nanoparticles are well crystallized. However, the product of the performed sonochemical synthesis contains CuSe as an additional component. It should be noted that all CIGSe, CIGS and CuSe are promising nanomaterials for applications in printed photovoltaics.

Acknowledgments

This work was partially supported by Institute of Physics — Center for Science and Education, Silesian University of Technology project no. BK-251/RIF/2014 and financial support for young scientists.

References

[1] D.L. Schulz, C.J. Curtis, R.A. Flitton, H. Wiesner, J. Keane, R.J. Matson, K.M. Jones, P.A. Parilla, R. Noufi, D.S. Ginley, *J. Electron. Mater.* **27**, 433 (1998).

[2] M. Kaelin, D. Rudmann, A.N. Tiwari, *Sol. Energy* **77**, 749 (2004).

[3] J.H. Lee, J. Chang, J.-H. Cha, Y. Lee, J.E. Han, D.-Y. Jung, E.Ch. Choi, B. Hong, *Eur. J. Inorg. Chem.* **2011**, 647 (2011).

[4] S.C. Choo, A.M. Etchells, L.A.K. Watt, *Phys. Rev. B* **4**, 4499 (1971).

[5] S. Kończak, K. Kotewicz, M. Nowak, *Phys. Status Solidi A* **65**, 447 (1981).

[6] M. Nowak, B. Kauch, P. Szperlich, *Rev. Sci. Instrum.* **80**, 046107 (2009).

[7] M. Nowak, Ł. Bober, B. Borkowski, M. Kępińska, P. Szperlich, D. Stróż, M. Sozańska, *Opt. Mater.* **35**, 2208 (2013).

[8] S.-H. Han, F.S. Hasoon, H.A. Al-Thani, A.M. Hermann, D.H. Levi, *J. Phys. Chem. Sol.* **66**, 1895 (2005).

[9] S.R. Gosavi, N.G. Deshpande, Y.G. Gudage, R. Sharma, *J. Alloys Comp.* **448**, 344 (2008).

[10] A. Rogalski, J. Piotrowski, *Prog. Quantum Electron.* **12**, 87 (1988).

[11] W.K. Metzger, I.L. Repins, M.A. Contreras, *Appl. Phys. Lett.* **93**, 022110 (2008).